Uptake and effects of orally ingested polystyrene microplastic particles in vitro and in vivo

Stock, Valerie; Böhmert, Linda; Lisicki, Elisa; Block, Rafael; Cara-Carmona, Julia; Pack, Laura Kim

Published in:
Archives of Toxicology

DOI:
10.1007/s00204-019-02478-7

Publication date:
2019

Document Version
Peer reviewed version

Uptake and effects of orally ingested polystyrene microplastic particles *in vitro* and *in vivo*

Valerie Stock[1,§], Linda Böhmert[1,§,*], Elisa Lisicki[1], Rafael Block[1], Julia Cara-Carmona[1], Laura Kim Pack[1], Regina Selb[1], Dajana Lichtenstein[1], Linn Voß[1], Colin J. Henderson[2], Elke Zabinsky[3], Holger Sieg[1], Albert Braeuning[1], Alfonso Lampen[1]

1 German Federal Institute for Risk Assessment, Max-Dohrn-Str. 8-10, 10589 Berlin, Germany

2 Systems Medicine, Jacqui Wood Cancer Centre, School of Medicine, University of Dundee, Ninewells Hospital, Dundee, DD1 9SY

3 Institute of Experimental and Clinical Pharmacology and Toxicology, University of Tübingen, Wilhelmstr. 56, 72074 Tübingen

[§]These authors contributed equally to the study

*Corresponding author:

Linda Böhmert, German Federal Institute for Risk Assessment, Max-Dohrn-Str. 8-10, 10589 Berlin, Germany. Phone: +49 (30) 18412-3718, E-mail: Linda.Boehmert@bfr.bund.de

KEYWORDS:

microplastic, oral uptake, particle size, gastrointestinal barrier, HOTT mice

ABSTRACT

Evidence exists that humans are exposed to plastic microparticles via diet. Data on intestinal particle uptake and health-related effects resulting from microplastic exposure are scarce. Aim of the study was to analyze the uptake and effects of microplastic particles in human *in vitro* systems and in rodents *in vivo*.

The gastrointestinal uptake of microplastics was studied *in vitro* using the human intestinal epithelial cell line Caco-2 and thereof-derived co-cultures mimicking intestinal M-cells and goblet cells. Different sizes of spherical fluorescent polystyrene particles (1, 4 and 10 μm) were used to study particle uptake and transport. A 28-days *in vivo* feeding study was conducted to analyze transport at the intestinal epithelium and oxidative stress response as a potential consequence of microplastic exposure. Male reporter gene mice were treated 3 times per week by oral gavage with a mixture of 1 μm ($4.55x10^7$ particles), 4 μm ($4.55x10^7$ particles) and 10 μm ($1.49x10^6$ particles) microplastics at a volume of 10 mL/kg/bw. Effects of particles on macrophage polarization were investigated using the human cell line THP-1 to detect a possible impact on intestinal immune cells.

Altogether, the results of the study demonstrate the cellular uptake of a minor fraction of particles. *In vivo* data show the absence of histologically detectable lesions and inflammatory responses. The particles did not interfere with the differentiation and activation of the human macrophage model. The present results suggest that oral exposure to polystyrene microplastic particles under the chosen experimental conditions does not pose relevant acute health risks to mammals.

INTRODUCTION

Global production of plastics has increased significantly over the last decades (PlasticsEurope 2016) and a further increase of use is expected (Jambeck et al. 2015; Sutherland et al. 2010). The most commonly produced types of polymers are polyethylene (PE), polypropylene (PP), and polystyrene (PS) with a relevant fraction of intentionally produced microplastics, commonly defined by a particle diameter of less than 5 mm (EFSA 2016). These so-called primary microplastics are mainly produced for cosmetic applications (Napper et al. 2015). Released from personal products (e.g. toothpaste) and cleaning agents, its remnants are transported to sewage systems and finally to the marine environment (Thompson 2015; van Wezel et al. 2016). Beside intentionally produced microplastics, other plastic items may be disposed and transported to the ocean. Plastics make up about 60 to 80 % of marine litter (Andrady 2003) and are decomposed by environmental factors like UV radiation, salt water and marine biota to so-called secondary microplastics (Cole et al. 2011; Hidalgo-Ruz et al. 2012). This has been described previously (Andrady 2003; Barnes et al. 2009; Lambert and Wagner 2016). Primary and secondary microplastics from the environment can enter the food chain and lead to oral exposure of humans. Based on a review of existing literature, the European Food Safety Agency (EFSA) concluded that a very minor fraction of particles smaller than 150 μm in diameter may cross the intestinal mucosal barrier, whereas only very small particles with a diameter smaller than 1.5 μm may be transported to deeper tissues (EFSA 2016). According to EFSA, data on toxicity, toxicokinetics and the presence of microplastics in food are still insufficient. Therefore, a reliable risk assessment of microplastics cannot be conducted yet (EFSA 2016).

The main adsorptive part of the gastrointestinal tract is the small intestine. Besides from absorbing nutrients, water and other compounds, it also provides a protective barrier for the organism. Several cell types compose the gastrointestinal epithelium: enterocytes, goblet cells, enteroendocrine cells, Paneth cells, microfold cells, cup cells, and tuft cells (Koeppen and Stanton 2017). The epithelial cell layer formed by enterocytes is connected by tight junctions and thus forms a physical barrier. Goblet cells secrete a mucus layer that protects the epithelium from luminal contents. Microfold cells, commonly referred to as M cells, transport antigens from the intestinal lumen to the basolateral side and deliver them to mucosa-associated lymphoid tissue (MALT). In the small intestine, M cells are associated with the Peyer's patches (Sarmento, 2015). Small polymer particles can be taken up from the gut by M cells, which transport them through the intestinal barrier. From there they may reach the lymphatic system, the liver and gall bladder. Particles are then re-released into the gut together with bile before excretion with feces (Galloway 2015; Jani et al. 1992b; Jepson et al. 1993).

The intestinal epithelium is also an important organ for the immune system. It is the broadest surface of the body that comes in close contact to a variety of substances and one might speculate that the fine-tuned intestinal immune balance might be disturbed by microplastics. Macrophages are immune cells which occur at high frequency in the intestine (Grainger et al. 2017; Santaolalla et al. 2011). They are essential for maintaining mucosal homeostasis and are located mostly in the lamina propria in close proximity to the epithelial monolayer in the gastrointestinal mucosa. Intestinal macrophages play an essential role by clearing apoptotic or senescent cells, inducing tissue remodeling, maintain tissue homeostasis, and thereby regulating the integrity of the epithelial barrier (Bain and Mowat 2014). They also establish and mediate tolerance towards the high burden of food and commensal antigens (Grainger et al. 2017). Furthermore, the location of macrophages enables them to capture and destroy any material breaching the epithelial barrier. While doing this, intestinal macrophages trigger pro-inflammatory responses by respiratory burst activity, generation of nitric oxide or inflammatory cytokines (Bain and Mowat 2014). Macrophages are key modulators and effector cells in the immune response and respond to microenvironmental signals by polarization. Polarization enables macrophages to act in a pro- or anti-inflammatory manner by the secretion of cytokines and the production of ROS, and can be described by the polarization stages M1 and M2. Functional polarization of macrophage occurs under physiological as well as pathological and is considered a key determinant of disease development and/or regression (Martinez and Gordon 2014; Sica et al. 2015).

The aim of this work was to quantify the intestinal uptake of different polystyrene microparticles *in vivo* and *in vitro*, by including different intestinal cell lines and an *in vivo* 28-days oral feeding study in heme-oxygenase-1 triple transgenic reporter mice in which oxidative stress can be visualized via a reporter enzyme. In addition, particle effects were investigated with a focus on the induction of oxidative stress, as a possible hallmark of unspecific stress induced by the presence of foreign particulate material in the organism. In addition, effects of microplastics on macrophage polarization were analyzed to account for potential effects of the particles on the immune system.

METHODS

Chemicals and microplastics:

Chemicals were purchased from Sigma-Aldrich (Taufkirchen, Germany), Merck (Darmstadt, Germany), or Carl Roth (Karlsruhe, Germany) if not otherwise indicated. The 1 μm polystyrene particles (FluoSpheres Polystyrene Carboxylated Microspheres, 1.0 μm) were purchased from

Thermo Fisher Scientific (Waltham, Massachusetts, USA) and the 4 μm and 10 μm polystyrene particles (PFL-4070, Sky Blue fluorescent particles, size 3.6 – 4.5 μm; and PFH-10056 Nile red fluorescent particles, size 10.0 – 14.0 μm) were purchased from Kisker Biotech GmbH (Steinfurt, Germany). All three particle types were provided with negatively charged surface modifications (1 μm: carboxy, 4 and 10 μm: sulfate).

Paricle characterization:

Particle sizes were verified by Dynamic Light Scattering with a Zetasizer Nano ZS (Malvern Panalytical GmbH, Kassel, Germany), and by confocal fluorescence microscopy (Leica TCS SP5, Leica Microsystems GmbH, Wetzlar, Germany) and ImageJ software (Laboratory for Optical and Computational Instrumentation (LOCI) of the University of Wisconsin-Madison, Madison, Wisconsin, USA). A complete z-stack was measured for at least 100 particles and merged to determine their maximum diameters by ImageJ. Results are given as histograms.

Cell culture:

Caco-2 (ECACC: 86010202) and HT-29 MTX E12 (ECACC: 12040401) cells were obtained from the European Collection of Authenticated Cell Cultures (Salisbury, UK). Raji B-lymphocytes (ATCC: CCL-86) were purchased from American Type Culture Collection (Manassas, Virginia, USA) and THP-1 cells were obtained from the Leibniz Institute DSMZ-German Collection of Microorganisms and Cell Cultures (DSMZ-No. ACC-16; Braunschweig, Germany). Caco-2 and human Raji B lymphocytes were cultured in Dulbecco's Modified Eagle Medium (DMEM; GE Healthcare, Freiburg, Germany) with 10 % FCS (fetal calf serum; Capricorn Scientific GmbH, Ebsdorfergrund, Germany) and 10^5 Units/l penicillin and 100 μg/mL streptomycin (P/S; PAA Laboratories GmbH, Pasching, Austria). The mucus-secreting cell line HT29-MTX was cultured in DMEM with 10 % FCS, 1 % P/S and 1 % non-essential amino acids (NEAA; PAA Laboratories GmbH, Pasching, Austria). THP-1 cells were cultured in RPMI 1640 medium with 10 % FCS and 1 % P/S. Adherent cell lines were kept semi-confluent in routine culture. Cells were cultivated at 37 °C and 5 % CO_2 and passaged every 2 to 3 days. Passaging of Caco-2 and HT29-MTX cells was performed by aspirating the culture medium, washing with phosphate-buffered saline (PBS) and incubating with trypsin-EDTA (0.05 %) in Dulbecco's Phosphate-Buffered Saline (DPBS) (1x) (Capricorn Scientific GmbH, Ebsdorfergrund, Germany) at 37 °C for 3-5 min (Caco-2) or 10 min (HT29-MTX). The process was

stopped by adding 10 mL of FCS-containing cell culture medium and cells were separated from the medium by centrifugation. Passaging of Raji B lymphocytes and THP-1 cells was performed by diluting a small amount of homogeneous cell suspension into new medium.

Cell viability:

Caco-2 cells were seeded in 96-well plates at a density of 5,000 cells per well and allowed to attach for 24 h. Cell culture medium was then replaced by 100 µL of phenol red-free medium containing different concentrations of the 1 µm, 4 µm and 10 µm particles. These selected sizes represent relevant sizes of microplastic and are small enough to be taken up by single cells. The maximum concentration of particles was determined by the stock concentration of particles and the need to delute in cellculture medium. Triplicate determinations were assayed per condition. After 24 h or 48 h, particles were removed by aspiration and 100 µL of phenol red-free medium was added. Cell viability was first measured by means of the Cell Titer Blue assay (CTB; Promega, Madison, Wisconsin, USA), measured according to the manufacturer's instructions on a multi-well plate reader (Tecan, Männedorf, Switzerland). Afterwards, the 3-(4,5-dimethylthiazole-2-yl)-2,5-diphenyltetrazolium bromide (MTT) assay was conducted in the same plates. Here, 10 µL of a 5 mg/mL solution of MTT in PBS was added for another hour. Subsequently, supernatants were removed and 130 µL desorption agent (0.7 % (w/v) sodium dodecyl sulfate (SDS) in isopropanol) was added. Plates were shaken for 30 min. Absorption was measured at 570 nm and background absorption (630 nm) was subtracted. Measurements were corrected for background signals (wells incubated with all assay components and particles, but without cells) by subtracting the values from wells incubated without cells and then related to the solvent control (set to 100 %). The background values were also used to determine particle-assay interferences. Means and standard deviations were calculated from at least three independent experiments.

Particle uptake studies using transwell systems:

Three different Caco-2-based *in vitro* models for the intestinal epithelium were used. All were cultured in 12-well transwell plates with inserts of 1.12 cm^2 growth area and a 3 µm pore size polycarbonate membrane (Corning Incorporated, New York City, New York, USA). For Caco-2 monoculture, 50,000 cells were seeded on the membrane and let differentiate for 3 weeks. The cell culture medium was changed every 2 to 3 days. For the mucus co-culture model, 40,000 Caco-2 cells

and 10,000 HT29-MTX cells were seeded at the same time on the membrane and let differentiate for 3 weeks. The cell culture medium was changed every 2 to 3 days. For the M-cell model, the protocol developed by des Rieux et al. was adapted as previously described (des Rieux et al. 2007; Lichtenstein et al. 2017a; Lichtenstein et al. 2017b): on day 1, 50,000 Caco-2 cells were seeded into the inserts. At day 7 to 8, the inserts were inverted; silicone tubes were attached to the basolateral side of the membranes and filled with culture medium. At day 16, 50,000 Raji B cells per well were added into the silicone tubes. At day 20, the inserts were taken off the box, tubes were removed and inserts were re-inverted and put back into 12-well plates. At this point, the transwell inserts were again in their initial position with the apical side upwards. At day 21, cells were exposed to the desired concentrations of particles.

Membrane integrity was checked by transepithelial electrical resistance (TEER) measurements as well as by fluorescein isothiocyanate–dextran (FITC-dextran) transport. TEER measurements were performed with an EVOM2 Electrode (World Precision Instruments, Sarasota, Florida USA) as described earlier (Lichtenstein et al. 2015). For the FITC-dextran measurements, 10 kDa dextran was added to the apical compartment (concentration of 1 mg/mL) and its transport was measured after incubation in the basolateral chamber via a Tecan Infinite 200 PRO plate reader (Tecan, Männedorf, Switzerland) at λ_{exc} = 485 nm and λ_{emm} = 535 nm. The apparent permeability coefficient (Papp) was calculated as described in detail in a recent publication (Lichtenstein et al. 2015).

After 21 days of differentiation, the cells in the transwell inserts were exposed to high but non-toxic concentrations of differently sized polystyrene microplastic particles, or to culture medium as a control, from the apical side in a volume of 500 µL cell culture medium. 500 µL fresh cell culture medium without particles was pipetted into the basolateral compartment and plates were incubated for 24 h. Afterwards, the basolateral and apical medium fractions, as well as the apical PBS washing fractions were collected and particle fluorescence was analyzed using the Tecan plate reader. To quantify the amount of particles, calibration curves were prepared from the same particles and matrices (cell culture media and PBS) as used in the incubations, starting with the initial particle concentrations. The lower limits of quantification (LLOQs) for each particle type were calculated by multiplying the standard deviation of five blank values (DMEM without particles) by nine. The transwell inserts including the cell monolayer were fixed with 3.7 % formaldehyde in PBS for half an hour and washed 3 times with PBS and then transferred to a new 12-well plate. Potentially absorbed particles were measured by fluorescence scan of the whole area of the transwell membrane and calculated by stepwise addition of a known amount of particles. To determine the amount of

particles present in the cells, the fluorescence of the transwell inserts was measured against a calibration curve of the respective particles.

Microscopic examinations:

In order to distinguish between particles on top or inside the cells, a confocal microscope was used. Cell monolayers from the transwell experiments were washed 3 times with PBS, permeabilized with the non-ionic surfactant Triton-X 100 for 20 min, washed again 3 times and stained with ActinGreen 488 stain (Life technologies, New York, USA) at 37 °C for 30 min. Then the membranes were washed again and cut out of the insert. With the cell layer upwards, the membranes were fixed on a coverslip using Kaiser's glycerin gelatin (Carl Roth GmbH + Co. KG, Karlsruhe, Germany) and let dry overnight. Three random sections per membrane were counted manually in order to receive a representative particle count. For each spot, the xzy acquisition mode was selected, which shows the membrane laterally from top of the cells (villi) to bottom (membrane), allowing a complete view of the cells. In this mode, a 301 µm trajectory line was scrolled through the z plane and the number of particles in or on the cells was counted. The Actin Green 488-stained cell membrane enabled a clear differentiation from the fluorescent particles inside or on top of the cells. The ratio of particles counted in/on the cells was calculated, and the previously obtained fluorescence of the membrane by the Tecan plate reader (see above) was used to calculate the fraction of particles in/on the cells in the whole membrane. Means and standard deviations were calculated from at least three independent experiments.

The differentiation of THP-1 monocytes into macrophages was examined microscopically (Zeiss, Axio Observer, Carl Zeiss, Jena, Germany) by determining the shape and adherence of the cells. After treatment with different polystyrene microplastic particles, their uptake by THP-1 monocytes polarized to macrophages was also checked by fluorescence microscopy.

Differentiation and polarization of THP-1 cells to M1 and M2 macrophages:

Differentiation of THP-1 cells into M0 macrophages was induced by 25 nM phorbol-12-myristate-13-acetate (PMA) for 24 h (Schwende et al. 1996; Tsuchiya et al. 1982). Afterwards, the cell culture medium was changed and cells were cultivated for another 24 h without PMA. During this period, cells were incubated with microplastic particles in concentration of 100,000 (1 µm), 250,000 (4 µm)

or 60,000 (10 μm) particles per mL medium. Afterwards, medium was changed again to induce polarization of macrophages to M1 and M2 stages. Induction of M1 macrophages was triggered by 20 ng/mL interferon gamma (IFNγ) and 0.1 μg/mL lipopolysaccharide (LPS), while induction of M2 macrophages was triggered by 20 ng/mL interleukin 4 and 13 (IL-4 and IL-13). Incubation was stopped by harvesting the cells for analysis after 30 min, 24 h or 72 h.

Western blotting:

THP-1 cells were harvested after washing by scraping and washing the cells pellet with PBS. Proteins were isolated using RIPA (radioimmunoprecipitation assay) buffer with protease and phosphatase inhibitors and sonification (10 sec. 2 times 10 % cycles; 25 % power; Sonopuls UW 2200, Bandelin Electronic GmbH & Co. KG, Berlin, Germany) on ice. Afterwards, samples were centrifuged for 30 min at 14,000 rpm (20,817 x g) and 4 °C, and the supernatant was used for analysis. The protein amount was determined by the Bicinchoninic Acid (BCA) assay using a bovine serum albumin (BSA) calibration curve. 10 μg of each sample in 10 μL (diluted with PBS) were heated to 70 °C for 10 min and separated by SDS-PAGE (BioRad Mini PROTEAN Tetra System, Bio-Rad Laboratories, Inc., Hercules, California, USA). Separated proteins were blotted to nitrocellulose membranes using the semi-dry method (TE 77 PWR Semi-Dry Transfer Unit, 21 × 26 cm, Amersham Biosciences, GE Healthcare GmbH, Solingen, Germany). The membranes were incubated over night at 4 °C with 5 % milk powder in Tris-buffered saline with Tween20 (TBST buffer) to block unspecific binding sites. Membranes were then incubated with primary antibodies against STAT1 (STAT1 Polyclonal Antibody (PA5-19858), Rabbit Anti-Human), pTyr701 phosphorylated STAT1 (Phospo-STAT1 pTyr (701) Antibody (15H13L67), Rabbit Anti-Human) and pTyr641 phosphorylated STAT6 (Phopho-STAT6 (Tyr641) Antibody (46H1L12), Rabbit Anti-Human). All antibodies were purchased from Thermofisher Scientific, Waltham, Massachusetts, USA, and incubated with the membranes at 1:1000 dilutions in TBST with 5 % BSA for 1 h at room temperature. Subsequently, a horseradish peroxidase (HRP)-conjugated secondary antibody (IgG-HRP mouse anti-rabbit (HAF008), R&D Systems, Inc., Minneapolis, Minnesota, USA) was incubated with the membrane for 2 h at 4 °C. Results were detected using the Super Signal West Femto Maximum Sensitivity Substrat Kit (Thermofisher Scientific, Waltham, Massachusetts, USA) and VersaDocTM Mp 4000 equipped with the Quantity One Software (Vers. 4.6.1; Bio-Rad Laboratories, Inc., Hercules, California, USA).

Quantitative real-time RT-PCR:

RNA was isolated using the RNeasy mini kit (Qiagen, Hilden, Germany). cDNA synthesis was performed with the High Capacity cDNA Reverse Transcription Kit (Applied Biosystems, Foster City, California, USA). For monitoring of the differentiation of M1 and M2 macrophages, the mRNAs encoding M1- or M2-specific chemokines and surface receptors (CXCL10, CCL22, CD206, CD209) were quantified using the Maxima SYBR Green/ROX qPCR Master Mix (Thermofisher Scientific, Waltham, Massachusetts, USA). Gene expression was measured on a MX3005P Stratagene thermal cycler via MXPro software (Agilent Technologies, Inc., Santa Clara, California, USA). Results were evaluated using the ΔΔCt method (Livak and Schmittgen 2001).

In vivo study:

Those carrying out animal work in this study did so with Personal and Project Licences granted by the UK Home Office under the Animals (Scientific Procedures) act (1986), as amended by EU Directive 2010/63/EU.

All animal work described in this study was carried with Personal and Project Licenses granted by the UK Home Office under the Animals (Scientific Procedures) act (1986), as amended by EU Directive 2010/63/EU after approval by the Welfare and Ethical treatment of Animals Committee of the University of Dundee and the University Veterinary Surgeon. All animals were supplied from the Medical School Resource Unit, University of Dundee, on a C57BL/6NTac background, held in open-top cages with ad libitum access to food (RM1, Special Diet Services, Stepfield, Witham, Essex, UK) and water, and a 12 h light/dark environment. Temperature and relative humidity were maintained between 20 °C and 24 °C, and 45 % and 65 %, respectively. Animals were inspected regularly by staff trained and experienced in small animal husbandry, with 24 h access to veterinary advice. Heme oxygenase-1 (Hmox) reporter mice were generated as previously described (McMahon et al. 2018). Male Hmox1 reporter mice (16-20 weeks, n=5 per group) were treated 3 times per week for 28 days by oral gavage with either vehicle (0.5 % (w/v) carboxymethylcellulose (CMC; Sigma Aldrich, Taufkirchen, Germany) or with a mixture of 1 μm (4.55×10^7 particles), 4 μm (4.55×10^7 particles) and 10 μm (1.49×10^6 particles) microplastics in CMC at a volume of 10 mL/kg body weight. As no reliable data on human exposure exist, and because the study was generally aimed at hazard identification, particle concentrations were chosen which are in the range of particle doses administered in previous studies (see Discussion section for details) which, however, are expected to

considerably exceed human exposure. The treatment scheme with 3 applications per week was chosen to account for a realistic scenario of some days with consumption of highly plastic-contaminated food followed by days without remarkable exposure. At the end of studies, all animals were killed by exposure to a rising concentration of CO_2 and death confirmed by exsanguination. The median lobe of the liver was fixed in 10 % neutral buffered formalin (Sigma Aldrich, Taufkirchen, Germany), while the small intestine – cut into duodenum, ileum and jejunum – and testes were fixed in 4 % (w/v) paraformaldehyde (Sigma Aldrich, Taufkirchen, Germany). Large intestine, lung, heart, spleen and kidneys were fixed in Mirsky's fixative (National Diagnostics, Atlanta, Georgia, USA). Tissues were stored at 4 °C, formalin-fixed tissues for 4h, Mirsky-fixed tissues overnight, before being transferred into 30 % (w/v) sucrose (Sigma Aldrich, Taufkirchen, Germany) for 24 h. Embedding was carried out in Shandon M-1 Embedding Matrix (Thermo Fisher Scientific, Waltham, Massachusetts, USA) in a dry ice–isopentane bath. Sectioning was performed on an OFT5000 cryostat (Bright Instrument Ltd, Bedfordshire, UK). All sections were cut at 10 µm thickness with a chamber temperature of −20 °C, except lung sections, which were cut at 12 µm thickness with a chamber temperature of −23 °C.

In situ β-galactosidase (β-gal) staining:

Sections were thawed at room temperature and rehydrated in PBS supplemented with 2 mM $MgCl_2$ (Sigma Aldrich, Taufkirchen, Germany) for 5 min before being incubated overnight at 37 °C in X-gal staining solution (PBS (pH 7.4) containing 2 mM $MgCl_2$, 0.01 % (w/v) sodium deoxycholate, 0.02 % (v/v) Igepal CA630, 5 mM potassium ferricyanide, 5 mM potassium ferrocyanide and 1 mg/mL 5-bromo-4-chloro-3-indolyl β-D-galactopyranoside), all purchased from Sigma Aldrich (Taufkirchen, Germany). On the following day, slides were washed in PBS, counterstained inNuclear FastRed (Vector Laboratories, Burlingame, California, USA) for 5 min, washed twice in distilled water and dehydrated through 70 % and 95 % ethanol before being incubated in Histoclear (VWR, Radnor, Pennsylvania, USA) for 3 min, air-dried and mounted in DPX mountant (Sigma Aldrich, Taufkirchen, Germany).

Statistical analysis:

For cell viability measurements statistical analysis was done by One Way ANOVA ($p<0.05$, compared to untreated controls).

For particle uptake in Caco-2 cell-based models statistical analysis was done by One Way ANOVA ($p<0.05$) for each particle size to test for differences in overall particle absorption (sum of particles inside and on the cells) between the 3 models.

For real-time RT-PCR results statistical analysis was done by One Way ANOVA ($p<0.05$, untreated M1 or M2 macrophages compared to M0 and microplastic-treated cells compared to untreated controls).

RESULTS

Characterization of microplastics:

Both DLS measurements and confocal imaging were conducted to experimentally determine the sizes of the different polystyrene particles (Figure 2): image analysis of the 1 µm particle revealed a mean size of 1.05 µm, while corresponding DLS analysis showed a mean size of 0.871 µm (Figure 2B-C). The respective sizes of the 4 µm particle were 3.99 µm (image analysis) and 3.809 µm (DLS), respectively (Figure 2B-C). The size of the 10 µm particles exceeded the detection limit of DLS and was therefore only assessed by image analysis which revealed a size of 9.78 µm.

Effects of microplastics on cell viability and growth of intestinal cells:

Cell viability of Caco-2 cells was measured by the Cell Titer Blue (CTB) and MTT assays after 24 and 48 h of incubation with microplastic particles (Figure 3). The highest possible concentrations of microplastic particles in the incubation medium were dictated by the concentrations of the particle stock dispersions, in order to avoid disturbance of cell growth by a lack of nutrients in the diluted medium. MTT assay results obtained after 48 h of incubation are representatively given in Figure 3 and plotted against different dose measures (particle number, particle mass, particle surface area and particle volume per incubation volume). Additional cell viability assays yielded comparable results and are presented as Supplemental Figure S1-S3. Supplemental Figure S4 gives an overview of the conversion of particle number, mass, surface area and volume for the individual particles. Cell

viability curves shown in Figure 3 demonstrate that a pronounced loss of cell viability occurred only in the presence of very high concentrations of the 1 μm particles. No pronounced cytotoxicity was observed with the larger particles. The three cell viability curves run in parallel when plotted against particle number, whereas other visualizations revealed that the 1 μm particles appeared to be more toxic to the cells, when particle mass, surface, or volume were taken into account (Figure 3B-E). It should be noted that the cells were entirely covered with non-physiologically high plastic particles at cytotoxic concentrations, as can be taken from the microscopic images shown in Figure 3E which give an impression of the coverage of cells at high particle concentrations.

Uptake of microplastics by *in vitro* models of the human intestinal epithelium:

In addition to potential cytotoxic effects of microplastic particles on intestinal cells, the cellular uptake of particles by the intestinal epithelium is of interest. Therefore, three different Caco-2-based models of the intestinal epithelium were used to investigate particle uptake: the classic Caco-2 monolayer, the M cell model containing uptake-specialized cells, and the mucus model presumably providing an additional barrier for the apical uptake of particles. Different particle numbers ($1x10^8$/mL for the 1 μm and 4 μm polystyrene particles, and $3x10^6$/mL for the 10 μm polystyrene particles) were chosen in order to reduce the big discrepancies between the applied particle surfaces and volumes when using the same numbers of the different particles per milliliter, as the particle surface is considered to be the biological most relevant dose metic. (Schmid and Stoeger 2016) The fraction of applied particles bound to the cell surface or present inside the cells was determined by plate reader measurements and confocal microscopy (see Methods section for details). Intracellular particle uptake into Caco-2 cells was clearly shown for the 1 μm (up to 0.8 % of total particle recovery) and especially for the 4 μm (up to 3.8 %) particles in all three models. Fewer of the 10 μm particles were taken up (up to 0.07 %) (Figure 4A). No differences were observed between the M Cell and the Mucus model for the 4 μm particles (~4.8 %), whereas the 1 μm particles were present at significantly higher numbers in the M Cell model (5.8 %), when the sum of particles inside the cells and adsorbed to the cell membrane from outside was considered. Both the 1 μm and 4 μm particles were recovered at significantly higher rates in the co-cultures, as compared to the Caco-2 monoculture.

The transport of 1 μm particles was quantified using the medium from the basolateral compartments. Please note that the larger particles were not able to cross the transwell membrane

due to the pore size of 3 μm, while larger pore sizes prevented the formation of an appropriate cell monolayer. For all three culture systems the transport of particles into the basolateral compartment was below the quantification limit of the method, which corresponded to 0.144 % of the applied amount of particles. Thus, less than 0.144 % of the 1 μm polystyrene particles had crossed the Caco-2 monolayer.

In vivo effects of repeated-dose microplastic exposure in mice

Data obtained so far indicated the absence of remarkable cytotoxicity *in vitro*, but an uptake of a minor fraction of particles into intestinal cells. A 28-day oral feeding study was conducted in order to obtain *in vivo* confirmation of the *in vitro* findings. More importantly, we aimed to analyze possible effects of the intestinal presence of plastic microparticles on inflammation- and oxidative stress-related processes, as the induction of such processes may constitute a plausible physiological reaction to the presence of otherwise not specifically toxic foreign particles. To this end, the *in vivo* study was conducted with transgenic mice expressing a lacZ reporter gene under the control of the inflammation- and redox stress-sensitive heme oxygenase 1 promoter (so-called HOTT mouse, (McMahon et al. 2018)). Mice were exposed to a mixture of the 1 μm, 4 μm and 10 μm microplastic particles by gavage three times a week: 10 μl per g body weight of a dispersion containing 2.5% (v/v) of the plastic particle mix in 0.5 % carboxymethyl cellulose were administered (see Methods section for details). All animals appeared healthy throughout the experiment and did not show clinical signs of illness or other potentially treatment-related symptoms. Similarly, no statistically significant effects of microplastic exposure on body and organ weights (liver, spleen, kidney, heart, lung, testes) were recorded at necropsy (data not shown). Histological examination of hematoxylin/eosin-stained intestinal tissue sections revealed normal tissue morphology without noticeable pathological findings (cp. images in Figure 5).

In the absence of clear-cut histopathological changes, tissue samples from different intestinal sections, liver, spleen and kidney were stained for activity of the β-galactosidase reporter. This was done in order to detect evidence for possible sub-clinical effects of microplastic exposure on inflammatory responses and/or conditions of oxidative injury. Images of stained slices of different intestinal sections as well as of other organs demonstrate the absence of substance-induced activation of the heme oxygenase 1-dependent reporter in microplastic-treated mice from our study (Figure 5). Basal reporter activities visible in kidney and spleen were similarly observed in mice treated with the

vehicle only, with variance between individual animals from a single group (Figure 5). In summary, reporter analyses did not reveal evidence for the occurrence of inflammation and/or oxidative stress following exposure of mice to polystyrene microparticles.

Intestinal tissue of mice from our microplastic feeding study was subsequently examined for the presence of particles. As exemplarily demonstrated in Figure 6 only a few particles were detected by fluorescence microscopy in the intestinal walls of the animals. This indicated that only a very minor fraction of particles was taken up into the tissue. Due to the very low number of particles detected, no quantitative analysis of particle uptake was performed. No particles were found in other organs (liver, spleen, kidney).

Effect of microplastic particles on the polarization of macrophages:

Even though no evidence for the induction of inflammatory responses was evident from the *in vivo* study, activation of macrophages as a rather un-specific biological response to the presence of foreign particulate matter was additionally analyzed using a human *in vitro* system. We therefore studied the effects of microplastic exposure on the differentiation of macrophages by the use of the THP-1 monocyte cell line, which can be differentiated into various cell types closely resembling physiologically occurring sub-populations of macrophages. Particle uptake into these cells was also investigated. Differentiation of THP-1 cells into M0, M1 and M2 macrophages was successful as documented by microscopic examination, determination expected changes in cell surface marker proteins and transcription factors and chemokines (see Supplementary data S5-S8).

As a first step, we examined the uptake of microplastic particles into M0 macrophages, prior to the induction of M1 and M2 polarization. To this end, 24 h of macrophage differentiation into M0 cells were followed by additional 24 h of microplastic exposure, followed by the induction of M1- or M2-specific differentiation. Microplastic uptake was quantified at 24 and 72 h after the induction of polarization. All three differently sized polystyrene particles were taken up by THP-1-derived macrophages (Figure 7A). A comparable pattern of particle uptake (4 μm > 1 μm > 10 μm) was observed for the cells at 24 and 72 h of polarization, and this qualitatively resembled the findings obtained with Caco-2 cells. Nonetheless, the quantity of particle uptake was much bigger in the macrophages, as compared to the intestinal cells (Figure 7A): the overall fractions of macrophages that had taken up particles were about 40 to 80 % for the 4 μm particles and only 10 to 20 % for the smaller and bigger particles.

Beside the particle uptake into the macrophages, the influence of the microplastic particles on the polarization process of macrophages was also analyzed (Figure 7B-E). For this purpose, microplastic-loaded M0 macrophages (see experiment above) were exposed to the appropriate stimuli to induce polarization into M1 or M2 macrophages, respectively (see Methods section for details). Western blotting analysis showed that after incubation with three different sizes of polystyrene microplastics, STAT-1 proteins were phosphorylated only in M1 macrophages and STAT-6 proteins only in M2 macrophages, to the same extent as in cells not previously exposed to microplastics. Thus, the tested polystyrene microplastic particles had no influence on the phosphorylation of STAT-1 and STAT-6, two prototype markers of macrophage polarization. Comparable results showing the absence of effects of microplastic exposure were yielded from real-time RT-PCR analysis of relative mRNA expression of the M1- and M2-typical chemokines (CXCL10 and CCL22) and surface receptors (CD209 and CD206) (Figure 7C). In summary, the data obtained with THP-1-derived macrophages show substantial uptake of the particles into the cells, but do not provide evidence for effects on macrophage polarization and/or chemokine release.

DISCUSSION

The aim of this project was to provide more detailed *in vivo* and *in vitro* information about the potential uptake and transport of microplastics through the human intestinal wall, and also about possibly resulting immunological and molecular effects. Findings from these investigations should help to close existing knowledge gaps on the uptake and toxicological effects of microplastics, as recently identified by EFSA (EFSA 2016).

Cytotoxicity was assessed by both CTB and MTT cell viability assays showing an increased cytotoxicity for 1 µm particles at the two highest concentrations while 4 µm and 10 µm particles were non-toxic. It is known that small particles have a higher bioreactivity due to their higher surface-to-volume ratio compared to bigger particles. This explains the higher cytotoxicity of the 1 µm particle compared to the 4 µm and 10 µm particles (Sharifi et al. 2012). The uptake and transport of plastics particles of different sizes were tested in three different *in vitro* systems mimicking the human gastrointestinal barrier: the classic Caco-2 monoculture, and coculture models with refined diversity and functionality using the additional cell lines Raji B (representing M cells) and HT29-MTX (representing goblet cells). Raji B lymphocytes integrate the immunologic and phagocytic function of the gut-associated lymphoid tissue (GALT), while mucus-producing HT29-MTX cells provide a

protection barrier also found in the digestive system. Additional uptake experiments were conducted with THP-1-derived macrophages. Our results suggest increased uptake into the cocultures, as compared to Caco-2 alone. Macrophages easily ingested polystyrene particles. Roughly consistent over all cell models, considerable uptake of the 1 µm and especially the 4 µm particles was shown, whereas cellular uptake of the larger 10 µm particles was much less efficient. This finding is consistent with earlier reports on size-dependent microplastic uptake where 10 µm has been set as the upper limit size for cellular uptake (Bruinink et al. 2015). Surprisingly, more 4 µm particles than 1 µm particles were found inside the cells. This may be explained by different import routes for the differently sized particles: macrophages and intestinal epithelial cells like Caco-2 are able to take up particles by phagocytosis or by pinocytosis/micropinocytosis. Cells can take up entities between 0.5 and 10 µm by phagocytosis, while particle uptake by pinocytosis and macropinocytosis may happen for particle sizes above 1 µm (Bruinink et al. 2015; Hirota and Terada 2012). Thus, 1 µm particles are likely absorbed by phagocytosis only, while 4 µm particles might be absorbed by phagocytosis and pinocytosis/macropinocytosis. An increased phagocytosis rate for particles between 2 and 4 µm was also shown by Champion et al. who investigated the dependence of phagocytosis on particle size in continuous alveolar rat macrophage cells (Champion et al. 2008). This may explain the increased internalization of 4 µm particles. Furthermore, unlike the 1 µm particles carrying a carboxy surface, the 4 µm particles carried sulfate groups, which may cause different behavior with respect to cellular uptake. Transport through the Caco-2 monolayer was only observed for a very minor, not quantifiable fraction of the 1 µm particles, whereas experimental limitations precluded testing of transport of larger particles to the basolateral compartment. Altogether, these findings are in line with previous results on particle uptake, as documented in the recent EFSA report where it is concluded that only particles smaller than 1.5 µm in diameter may penetrate the gastrointestinal barrier be distributed to deeper organs (EFSA 2016).

Results from our *in vivo* study show little presence of particles in cells of the jejunum and duodenum. No particles were found in other organs. Previous articles describe the presence of 3 µm microplastic particles on the mucosal surface, within enterocytes and microvilli after oral administration in rats (Jani et al. 1992a). The maximum particle size taken up by the Peyer's patches was 1 µm in an earlier study (Jani et al. 1992b), so that the 4 µm and 10 µm particles were probably too large for efficient uptake. Furthermore, it was found that smaller particles (0.05, 0.3 and 1 µm) migrated into the serosal layers of the Peyer's patches, transversing the mesentery lymph vessels, lymph nodes and liver vessels (Jani et al. 1989; Jepson et al. 1993; Smyth et al. 2008). Another publication showed negatively

charged 50 nm polystyrene nanoparticles in lung, testis, spleen kidney and heart after oral administration (Walczak et al. 2015). Differences between the findings obtained in the different studies might be caused by the chosen dosage of particles: Jani and colleagues used 12.5 mg/kg body weight of their plastic particles, administered daily for ten consecutive days, and Walczak et al. used a single dose of 125 mg/kg body weight. In our particle mix we used approximately 1.25 mg/kg body weight for the 1 μm particles, 25 mg/kg body weight for the 4 μm particles, and 34 mg/kg body weight for the 10 μm particles three times a week for 28 days. Thus, both the treatment periods and the particle concentrations differ between previous publications and our experimental design. Especially the small 1 μm particles were administered in much lower doses in our trial. Moreover, our experimental approach with an application of particles three times per week diverges from previous studies. This protocol was chosen to more realistically reflect assumed exposure patterns of humans, for example by the ingestion of highly contaminated food on some days, followed by days without such exposure. Even though no precise calculation of human oral exposure to microplastics is possible based on the lack of data for most types of foodstuff, we are aware that the concentrations used in our rodent study were still orders of magnitude higher than what might be realistically expected for humans. In this context it should be noted that results from a study by Seifert and co-workers suggest that the uptake rate of particles is substantially correlated with the administered dose of particles: after direct administration of 3.7×10^5 particles (1 μm diameter, polystyrene) into the duodenum, 18 particles were detected in the lymph (not clearly stating whether this number refers to the sum of particles detected in the entire group of 5 animals or to the mean number of particles per animal), while this number rose to 775 particles up after application of 3.7×10^9 of particles (Seifert et al. 1996). In our study, the individual doses for each particle ranged between 1.49×10^6 and 4.55×10^7, so that the low uptake we observed appears plausible based on the lower doses, as compared to other publications. The dose-dependency of intestinal particle absorption (Seifert et al. 1996) should be taken into account when extrapolating findings from animal studies to the situation in humans. Uncertainty remains with respect to the question, if and how parameters such as particle material, shape, and surface modifications influence the gastrointestinal uptake of microplastics. Nonetheless, it can be concluded from the available data that only a very minor fraction of small microplastic particles enters the intestinal wall. Patients with diseases which increment the permeability of the gut wall, such as for example inflammatory bowel diseases, celiac disease, food allergies, or irritable bowel syndrome, may display altered bioavailability of microplastics. Data on putative long-term particle accumulation and agglomeration of such particles

inside the body are lacking. With respect to the intestinal wall, however, it might be assumed that the rapid physiological turnover of intestinal epithelial cells will eliminate most of the particles which have been taken up intracellularly. While most of the available literature points towards a very low oral bioavailability of microplastic particles, as reviewed by EFSA, data from a previous study by Deng and co-workers suggest that high numbers of 5 μm and 20 μm polystyrene particles cross the intestinal barrier and are distributed to deeper organs (Deng et al. 2017; EFSA 2016). However, the findings from the above study appear questionable due to the fact that the numbers of particles detected in the organs massively exceed the numbers of particles applied during the study. This problem has been addressed in a recent publication in more detail (Braeuning 2018) and prevents the use of the data from the Deng et al. study for a credible estimation of microplastic bioavailability (Deng et al. 2017).

With respect to toxicologically relevant effects of polystyrene microparticles, data from our *in vivo* study do not provide any evidence of histologically detectable adverse effects. Previous studies on the toxicity on microplastic particles have mainly focused on aquatic organisms and some effects have been reported in that context (Canesi et al. 2015; Della Torre et al. 2014; Lu et al. 2016; Rochman et al. 2014). Relevance of these findings for mammalian organisms is unclear. Moreover, our *in vivo* reporter analyses in transgenic mice suggest the absence of particle-induced oxidative stress and inflammation, which is in line with our *in vitro* findings of the lack of *in vitro* cytotoxicity of polystyrene microparticles and especially the lack of influence on macrophage differentiation and polarization. Inflammation and phagocyte activation were specifically chosen for investigation because they represent plausible endpoints of an early phase of unspecific damage by particulate matter (Khalili Fard et al. 2015). The apparent lack of toxicity of plastic particles is in line with the assumption that chemically rather inert polymers are not expected to exert pronounced cellular toxicity per se. Previous studies conducted in mammalian organisms aimed to analyze the gastrointestinal uptake of microplastics do not contain descriptions of unexpected toxicity in the experimental animals (Sinnecker et al. 2014; Walczak et al. 2015). This corroborates our present results and supports the assumption that exposure to environmental concentrations of microplastic particles does not bear a remarkable potential to exert toxic effects. It should be noted that polystyrene microparticle cytotoxicity has been reported at concentrations of 0.5 mg/mL of 3.5 μm particles in murine cells and at the same concentration of 1 μm particles in human THP-1 cells (Olivier et al. 2003; Prietl et al. 2014). These data are not at odds with our results, as the particle

concentrations used for incubation with macrophages corresponded to a maximum of 33 μg/mL for the biggest particles with a diameter of 10 μm.

Nonetheless, data gaps remain, not only with respect to possible differential effects of particles varying in size and material (especially nano-sized materials are of special interest here). Again, the abovementioned publication by Deng et al. should be discussed here: the authors conclude that data from mice exposed to microplastic particles suggest widespread health risks (Deng et al. 2017). However, adversity of the findings at the biochemical level, i.e. alterations in a number of metabolites, remains unclear, and issues with the validity of histopathological analyses from that group have been addressed previously (Baumann et al. 2016; Braeuning 2018). In conjunction with the aforementioned issues with the credibility of the uptake data, data from the study by Deng and colleagues appear not suited for the assessment of possible health effects of microplastics in mammalian organisms. Another very recent publication deals with effects of 5 μm and 50 μm polystyrene particles on intestinal mucus, hepatic lipid metabolism and gut microbiota (Lu et al. 2018). In the latter study, microplastics have been administered via the drinking water. Unfortunately, the study does not contain information about water and food consumption of the animals which would be needed to exclude that the effects observed were caused by differences in food or water uptake (as palatability of the water may have been changed by the microplastics). Analyses of mineral water for human consumption have revealed concentrations of up to 250 plastic microparticles per liter (Schymanski et al. 2018). A comparison of the latter value with the particle concentration of about $1.5*10^{10}$ of the 5 μM particles per liter in the study by Lu and co-workers (Lu et al. 2018) demonstrates that their findings were obtained at unphysiologically high particle exposure which does not allow for inference to possible risks for humans.

Besides possible risks directly conveyed by the particles, additional health concerns may arise from the scenario that hydrophobic contaminants adsorb to the particles, thus leading to altered uptake of the respective contaminants and/or to modulation of their bioavailability (Frias et al. 2010; Gauquie et al. 2015; Teuten et al. 2007). Similarly, the surface of microplastic particles may be colonized by microorganisms. Future research is needed to close the still existing knowledge gaps related to microplastic exposure and effects. The present data indicate that polystyrene particle uptake occurs only at a very low level and is not linked to remarkable toxicity. Nonetheless, clarification needs to be provided on the influence of parameters such as particle size, shape, material, adsorbed contaminants and microorganisms. Other types of microplastics such as PET or PE might exert behavior different from polystyrene. Similarly, future studies are needed to elucidate human microplastic exposure in

more detail in order to facilitate a conclusive risk assessment. At the current stage of research, however, available data indicate that orally ingested microplastic particles do not pose major health risks to the consumer.

ACKNOWLEDGMENT

The authors thank Anja Köllner and Beatrice Rosskopp for technical assistance. This work was supported by the German Federal Institute for Risk Assessment (projects 1322-675, 1322-622 and 1323-102).

DECLARATION OF INTEREST STATEMENT

We declare no conflict of interest.

REFERENCES

Andrady AL. 2003. Plastic litter and other marine debris. In: Plastics and the environment, (L. AA, ed). New York:John Wiley & Sons, 381-382.

Bain CC, Mowat AM. 2014. Macrophages in intestinal homeostasis and inflammation. Immunological reviews 260:102-117. PMC4141699. 10.1111/imr.12192.

Barnes DKA, Galgani F, Thompson RC, Barlaz M. 2009. Accumulation and fragmentation of plastic debris in global environments. Philosophical Transactions of the Royal Society B: Biological Sciences 364:1985-1998. 10.1098/rstb.2008.0205.

Baumann L, Schmidt-Posthaus H, Segner H, Wolf JC. 2016. Comment on "uptake and accumulation of polystyrene microplastics in zebrafish (danio rerio) and toxic effects in liver". Environmental science & technology 50:12521-12522. 10.1021/acs.est.6b04193.

Braeuning A. 2018. Uptake of microplastics and related health effects: A critical discussion of deng et al., scientific reports 7:46687, 2017. Archives of toxicology. 10.1007/s00204-018-2367-9.

Bruinink A, Wang J, Wick P. 2015. Effect of particle agglomeration in nanotoxicology. Archives of toxicology 89:659-675. 10.1007/s00204-015-1460-6.

Canesi L, Ciacci C, Bergami E, Monopoli MP, Dawson KA, Papa S, et al. 2015. Evidence for immunomodulation and apoptotic processes induced by cationic polystyrene nanoparticles in the hemocytes of the marine bivalve mytilus. Marine environmental research 111:34-40. 10.1016/j.marenvres.2015.06.008.

Champion JA, Walker A, Mitragotri S. 2008. Role of particle size in phagocytosis of polymeric microspheres. Pharmaceutical research 25:1815-1821. 10.1007/s11095-008-9562-y.

Cole M, Lindeque P, Halsband C, Galloway TS. 2011. Microplastics as contaminants in the marine environment: A review. Marine Pollution Bulletin 62:2588-2597. http://doi.org/10.1016/j.marpolbul.2011.09.025.

Della Torre C, Bergami E, Salvati A, Faleri C, Cirino P, Dawson KA, et al. 2014. Accumulation and embryotoxicity of polystyrene nanoparticles at early stage of development of sea urchin embryos paracentrotus lividus. Environmental science & technology 48:12302-12311. 5260196. 10.1021/es502569w.

Deng Y, Zhang Y, Lemos B, Ren H. 2017. Tissue accumulation of microplastics in mice and biomarker responses suggest widespread health risks of exposure. Scientific Reports 7:46687. 28436478. 10.1038/srep46687 https://www.nature.com/articles/srep46687#supplementary-information.

des Rieux A, Fievez V, Theate I, Mast J, Preat V, Schneider YJ. 2007. An improved in vitro model of human intestinal follicle-associated epithelium to study nanoparticle transport by m cells. European journal of pharmaceutical sciences : official journal of the European Federation for Pharmaceutical Sciences 30:380-391. 17291730. 10.1016/j.ejps.2006.12.006.

EFSA. 2016. Presence of microplastics and nanoplastics in food, with particular focus on seafood. EFSA Journal 14. 10.2903/j.efsa.2016.4501.

Frias JP, Sobral P, Ferreira AM. 2010. Organic pollutants in microplastics from two beaches of the portuguese coast. Mar Pollut Bull 60:1988-1992. 20800853. 10.1016/j.marpolbul.2010.07.030.

Galloway TS. 2015. Micro- and nano-plastics and human health. In: Marine anthropogenic litter, (Bergmann M, Gutow L, Klages M, eds). Cham:Springer International Publishing, 343-366.

Gauquie J, Devriese L, Robbens J, De Witte B. 2015. A qualitative screening and quantitative measurement of organic contaminants on different types of marine plastic debris. Chemosphere 138:348-356. 26126190. 10.1016/j.chemosphere.2015.06.029.

Grainger JR, Konkel JE, Zangerle-Murray T, Shaw TN. 2017. Macrophages in gastrointestinal homeostasis and inflammation. Pflugers Archiv : European journal of physiology 469:527-539. PMC5362667. 10.1007/s00424-017-1958-2.

Hidalgo-Ruz V, Gutow L, Thompson RC, Thiel M. 2012. Microplastics in the marine environment: A review of the methods used for identification and quantification. Environmental science & technology 46:3060-3075. 22321064. 10.1021/es2031505.

Hirota K, Terada H. 2012. Endocytosis of particle formulations by macrophages and its application to clinical treatment:INTECH Open Access Publisher.

Jambeck JR, Geyer R, Wilcox C, Siegler TR, Perryman M, Andrady A, et al. 2015. Plastic waste inputs from land into the ocean. Science 347:768-771. 25678662. 10.1126/science.1260352.

Jani P, Halbert GW, Langridge J, Florence AT. 1989. The uptake and translocation of latex nanospheres and microspheres after oral administration to rats. The Journal of pharmacy and pharmacology 41:809-812. 2576440. https://doi.org/10.1111/j.2042-7158.1989.tb06377.x.

Jani PU, Florence AT, McCarthy DE. 1992a. Further histological evidence of the gastrointestinal absorption of polystyrene nanospheres in the rat. International Journal of Pharmaceutics 84:245-252. https://doi.org/10.1016/0378-5173(92)90162-U.

Jani PU, McCarthy DE, Florence AT. 1992b. Nanosphere and microsphere uptake via peyer's patches: Observation of the rate of uptake in the rat after a single oral dose. International Journal of Pharmaceutics 86:239-246. https://doi.org/10.1016/0378-5173(92)90202-D.

Jepson MA, Simmons NL, Savidge TC, James PS, Hirst BH. 1993. Selective binding and transcytosis of latex microspheres by rabbit intestinal m cells. Cell and tissue research 271:399-405. 8472299. https://doi.org/10.1007/BF02913722.

Khalili Fard J, Jafari S, Eghbal MA. 2015. A review of molecular mechanisms involved in toxicity of nanoparticles. Advanced pharmaceutical bulletin 5:447-454. 26819915. 10.15171/apb.2015.061.

Koeppen BM, Stanton BA. 2017. Functional anatomy and general principles of regulation in the gastrointestinal tract. In: Berne & levy physiology, Vol. 7, (Koeppen BM, Stanton BA, eds). Oxford:Elsevier Health Sciences, 511.

Lambert S, Wagner M. 2016. Formation of microscopic particles during the degradation of different polymers. Chemosphere 161:510-517. 27470943. 10.1016/j.chemosphere.2016.07.042.

Lichtenstein D, Ebmeyer J, Knappe P, Juling S, Bohmert L, Selve S, et al. 2015. Impact of food components during in vitro digestion of silver nanoparticles on cellular uptake and cytotoxicity in intestinal cells. Biological chemistry 396:1255-1264. 26040006. 10.1515/hsz-2015-0145.

Lichtenstein D, Ebmeyer J, Meyer T, Behr A-C, Kästner C, Böhmert L, et al. 2017a. It takes more than a coating to get nanoparticles through the intestinal barrier in vitro. European Journal of Pharmaceutics and Biopharmaceutics 118:21-29. 27993735 https://doi.org/10.1016/j.ejpb.2016.12.004.

Lichtenstein D, Meyer T, Böhmert L, Juling S, Fahrenson C, Selve S, et al. 2017b. Dosimetric quantification of coating-related uptake of silver nanoparticles. Langmuir 33:13087-13097. 28918629. 10.1021/acs.langmuir.7b01851.

Livak KJ, Schmittgen TD. 2001. Analysis of relative gene expression data using real-time quantitative pcr and the 2−δδct method. Methods 25:402-408. 11846609. https://doi.org/10.1006/meth.2001.1262.

Lu L, Wan Z, Luo T, Fu Z, Jin Y. 2018. Polystyrene microplastics induce gut microbiota dysbiosis and hepatic lipid metabolism disorder in mice. The Science of the total environment 631-632:449-458. 29529433. 10.1016/j.scitotenv.2018.03.051.

Lu Y, Zhang Y, Deng Y, Jiang W, Zhao Y, Geng J, et al. 2016. Uptake and accumulation of polystyrene microplastics in zebrafish (danio rerio) and toxic effects in liver. Environmental science & technology 50:4054-4060. 26950772. 10.1021/acs.est.6b00183.

Martinez FO, Gordon S. 2014. The m1 and m2 paradigm of macrophage activation: Time for reassessment. F1000prime reports 6. 24669294. 10.12703/P6-13.

McMahon M, Ding S, Acosta-Jimenez LP, Frangova TG, Henderson CJ, Wolf CR. 2018. Measuring in vivo responses to endogenous and exogenous oxidative stress using a novel haem oxygenase 1 reporter mouse. The Journal of physiology 596:105-127. 29086419. 10.1113/JP274915.

Napper IE, Bakir A, Rowland SJ, Thompson RC. 2015. Characterisation, quantity and sorptive properties of microplastics extracted from cosmetics. Marine Pollution Bulletin 99:178-185. 26234612. https://doi.org/10.1016/j.marpolbul.2015.07.029.

Olivier V, Duval JL, Hindie M, Pouletaut P, Nagel MD. 2003. Comparative particle-induced cytotoxicity toward macrophages and fibroblasts. Cell biology and toxicology 19:145-159. 12945743. https://doi.org/10.1023/A:1024723326036.

PlasticsEurope. 2016. Plastics - the facts 2016: An analysis of european plastics production, demand and waste data. [accessed 22/01/2018.

Prietl B, Meindl C, Roblegg E, Pieber TR, Lanzer G, Frohlich E. 2014. Nano-sized and micro-sized polystyrene particles affect phagocyte function. Cell biology and toxicology 30:1-16. PMC4434214. 10.1007/s10565-013-9265-y.

Rochman CM, Kurobe T, Flores I, Teh SJ. 2014. Early warning signs of endocrine disruption in adult fish from the ingestion of polyethylene with and without sorbed chemical pollutants from the marine environment. The Science of the total environment 493:656-661. 24995635. 10.1016/j.scitotenv.2014.06.051.

Santaolalla R, Fukata M, Abreu MT. 2011. Innate immunity in the small intestine. Current opinion in gastroenterology 27:125-131. 21248635. 10.1097/MOG.0b013e3283438dea.

Schwende H, Fitzke E, Ambs P, Dieter P. 1996. Differences in the state of differentiation of thp-1 cells induced by phorbol ester and 1,25-dihydroxyvitamin d3. Journal of leukocyte biology 59:555-561.

Schymanski D, Goldbeck C, Humpf HU, Furst P. 2018. Analysis of microplastics in water by micro-raman spectroscopy: Release of plastic particles from different packaging into mineral water. Water research 129:154-162. 29145085. 10.1016/j.watres.2017.11.011.

Seifert J, Haraszti B, Sass W. 1996. The influence of age and particle number on absorption of polystyrene particles from the rat gut. Journal of anatomy 189 (Pt 3):483-486. 8982820.

Sharifi S, Behzadi S, Laurent S, Forrest ML, Stroeve P, Mahmoudi M. 2012. Toxicity of nanomaterials. Chemical Society reviews 41:2323-2343. 10.1039/c1cs15188f.

Sica A, Erreni M, Allavena P, Porta C. 2015. Macrophage polarization in pathology. Cellular and molecular life sciences : CMLS 72:4111-4126. 26210152. 10.1007/s00018-015-1995-y.

Sinnecker H, Krause T, Koelling S, Lautenschlager I, Frey A. 2014. The gut wall provides an effective barrier against nanoparticle uptake. Beilstein journal of nanotechnology 5:2092-2101. 25551037. 10.3762/bjnano.5.218.

Smyth SH, Feldhaus S, Schumacher U, Carr KE. 2008. Uptake of inert microparticles in normal and immune deficient mice. Int J Pharm 346:109-118. 17723283. 10.1016/j.ijpharm.2007.06.049.

Sutherland WJ, Clout M, Côté IM, Daszak P, Depledge MH, Fellman L, et al. 2010. A horizon scan of global conservation issues for 2010. Trends in Ecology & Evolution 25:1-7. 19939492. 10.1016/j.tree.2009.10.003.

Teuten EL, Rowland SJ, Galloway TS, Thompson RC. 2007. Potential for plastics to transport hydrophobic contaminants. Environmental science & technology 41:7759-7764. 18075085. 10.1021/es071737s.

Thompson RC. 2015. Microplastics in the marine environment: Sources, consequences and solutions. In: Marine anthropogenic litter, (Bergmann M, Gutow L, Klages M, eds). Cham:Springer International Publishing, 185-200.

Tsuchiya S, Kobayashi Y, Goto Y, Okumura H, Nakae S, Konno T, et al. 1982. Induction of maturation in cultured human monocytic leukemia cells by a phorbol diester. Cancer research 42:1530-1536.

van Wezel A, Caris I, Kools SA. 2016. Release of primary microplastics from consumer products to wastewater in the netherlands. Environmental toxicology and chemistry 35:1627-1631. 26627661. 10.1002/etc.3316.

Walczak AP, Hendriksen PJ, Woutersen RA, van der Zande M, Undas AK, Helsdingen R, et al. 2015. Bioavailability and biodistribution of differently charged polystyrene nanoparticles upon oral exposure in rats. Journal of nanoparticle research : an interdisciplinary forum for nanoscale science and technology 17:231. PMC4440892. 10.1007/s11051-015-3029-y.

FIGURE LEGENDS

Figure 1: Schematic overview of the experimental approach. Particle uptake was studied *in vitro* using different Caco-2-based models of the human gastrointestinal epithelium. Particle uptake and effects were analyzed *in vivo* using a transgenic mouse model expressing a LacZ reporter under the control of the oxidative stress-responsive heme oxygenase 1 (Hmox1) promoter. *In vitro* effects of microplastics on macrophage polarization were investigated in human THP-1 cells.

Figure 2: Characterization of fluorescent 1 μm, 4 μm and 10 μm polystyrene (PS) particles by confocal microscopy with subsequent size determination by image analysis and by Dynamic Light Scattering (DLS). (**A**) Confocal images of fluorescent negatively charged 1 μm (left), 4 μm (middle), and 10 μm (right) polystyrene particles. (**B**) Size distributions of particle diameters, as determined by image analysis. (**C**) DLS curves for the 1 μm polystyrene (left) and 4 μm polystyrene (middle) particles. The size of the 10 μm particles exceeded the detection limit of the method and was therefore not determined.

Figure 3: MTT cell viability measurements in Caco-2 cells after 48 h of incubation with 1 μm, 4 μm and 10 μm polystyrene (PS) particles. (**A** to **D**) MTT assay cell viability measurements of proliferating Caco-2 cells after 48 h of incubation with three different sizes of microplastic particles. Results are given as percentage of the viability of the medium control. Mean values ± SD of n=3 independent

experiments are given. Statistical analysis was done by One Way ANOVA. (*p<0.05, compared to untreated controls) Cell viability curves are plotted against different dose measures: (**A**) particle number per incubation volume, (**B**) particle mass per incubation volume, (**C**) particle surface area per incubation volume and (**D**) particle volume per incubation volume. (**E**) Fluorescence-microscopic images of semi-confluent Caco-2 cells incubated with increasing particle concentrations demonstrate coverage of cells with particles at high concentrations. Top row: 1 µm polystyrene particles; middle row: 4 µm polystyrene particles; bottom row: 10 µm polystyrene particles.

Figure 4: Uptake of fluorescent 1 µm, 4 µm and 10 µm polystyrene (PS) microplastic particles into intestinal epithelial Caco-2 cells and their co-cultures after 24 h of incubation in a transwell system. (**A**) Percentage of microplastic particles found to interact with the cells of the Caco-2 monocultures, the M cell model, or the mucus model, as determined by confocal microscopy and plate reader-based fluorescence measurements. After counting of the particles inside and on top of the cells, the ratio of particles counted in/on the cells was calculated. Total fluorescence of the membrane was determined by the use of a plate reader and from that, the fractions of particles in/on the cells were calculated for the whole membrane. Particles which were found in the cytoplasm or on the basolateral side of the cell monolayer were counted as the "inside cells" fraction, while particles which were not absorbed by the cells but interacted with the microvilli were counted as the "on the cells" fraction. Mean values ± SD of n=3 independent experiments are given. (**B**) Representative confocal microscopic images of epithelial cells from the Caco-2 monoculture model incubated with the three different fluorescent microplastic particles (left: 1 µm polystyrene, middle: 4 µm polystyrene, right: 10 µm polystyrene). Cell membranes were stained with actin-green. * Differences in overall particle absorption (sum of particles inside and on the cells) between the 3 models were calculated by One-way ANOVA; p<0.05 in separate calculations for each particle size.

Figure 5: Histochemical staining for the activity of the oxidative stress and inflammation reporter enzyme β-galactosidase in transgenic mice treated with repeated doses of a mixture of microplastic particles for 28 days. The reporter enzyme is expressed under the control of the heme oxygenase 1 promoter (HOTT mouse). (**A**) Representative images from staining of the large intestine, duodenum, jejunum, ileum, kidney, spleen and liver are shown in comparison to mice having received only the

vehicle control. Tissues were counterstained by hematoxylin/eosin (HE). Staining of a $CdCl_2$-treated liver from a previous experiment is presented a positive control for β-galactosidase activity. Please note that differences in blue background staining result from differences in HE counterstaining, not from differences in β-galactosidase activities. (**B**) Enhanced display details of stainings from microplastic-treated mice showing histologically intact tissue from different organs and the absence of β-galactosidase staining.

Figure 6: Representative confocal images of 1 µm particles taken up into the (**A**) jejunal and (**B**) duodenal wall of a HOTT mouse fed with a mixture of three differently-sized fluorescent polystyrene particles (1 µm, 4 µm, 10 µm) three times a week for 28 days. Only a small number of individual particles were detectable in the tissue.

Figure 7: Microplastic particle uptake into THP-1-derived macrophages and influence of microplastics on macrophage differentiation. THP-1 monocytes were differentiated into M0 macrophages for 24 h with 25 nM PMA and then incubated with polystyrene microplastic particles during a 24 h resting phase. This was followed by the induction of M1- or M2-specific polarization. After 24 or 72 of the polarization phase, particle uptake, protein phosphorylation and gene expression were analyzed. (**A**) Particle uptake was determined by analysis of phase contrast and fluorescence-microscopic images of cells exposed to polystyrene microplastic particles. (**B** and **C**) Influence of the uptake of 1 µm, 4 µm and 10 µm polystyrene microplastic particles on the phosphorylation of STAT-1 and STAT-6 proteins in M0, M1 and M2 macrophages. Phosphorylated STAT proteins and loading control (Ponceau red staining) are shown. (**D** and **E**) Relative expression of M1 and M2 macrophage-specific chemokines and surface receptors in polystyrene-treated cells and controls after 24 h and 72 h of polarization determined by real-time RT-PCR. Mean values ± SD of n=3 independent experiments are given. #One Way ANOVA $p<0.05$, untreated M1 or M2 macrophages compared to M0. * One Way ANOVA $p<0.05$, microplastic-treated cells compared to untreated controls.

Figure 1

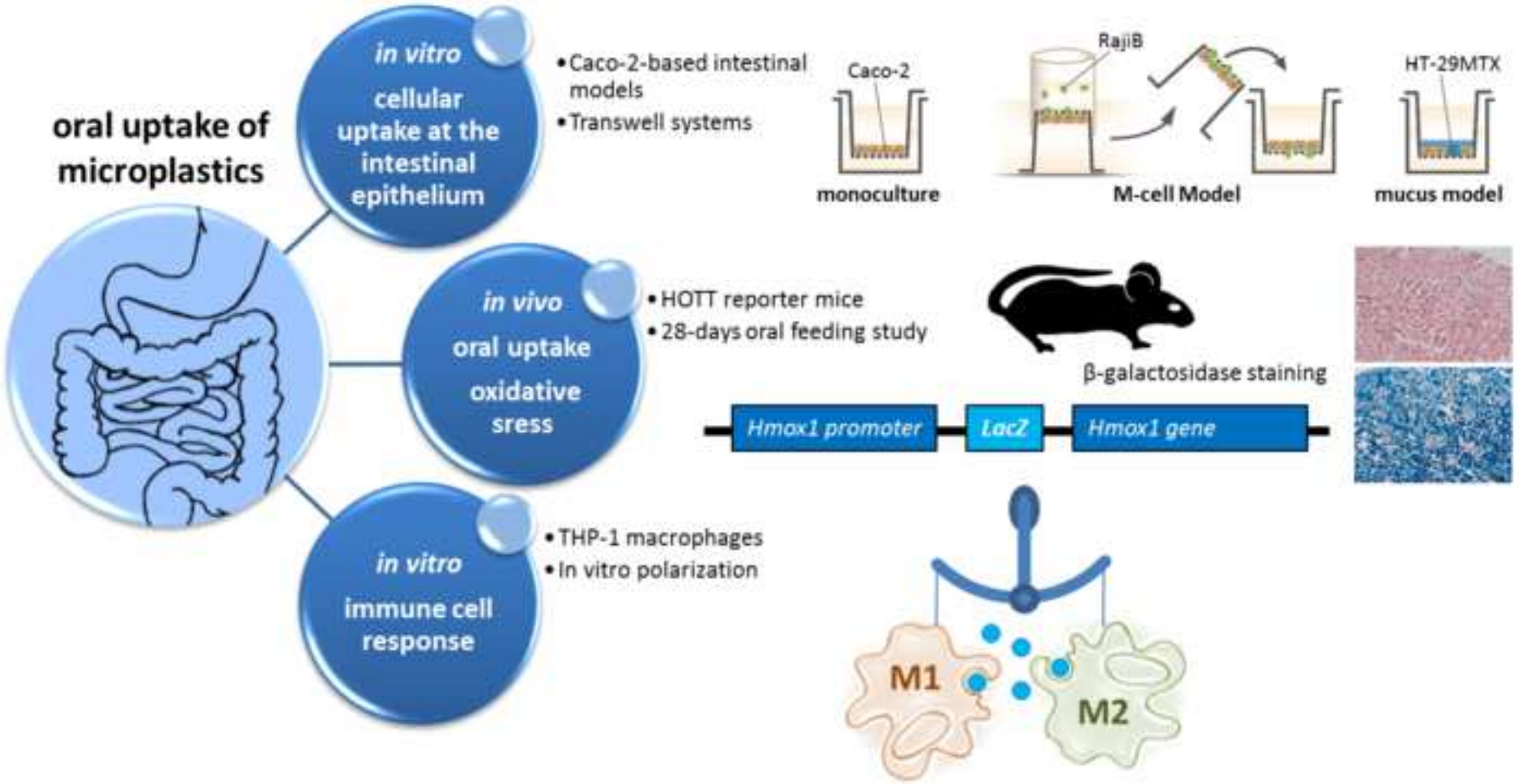

Figure 2

Click here to access/download;Figure;Figure 2.tif

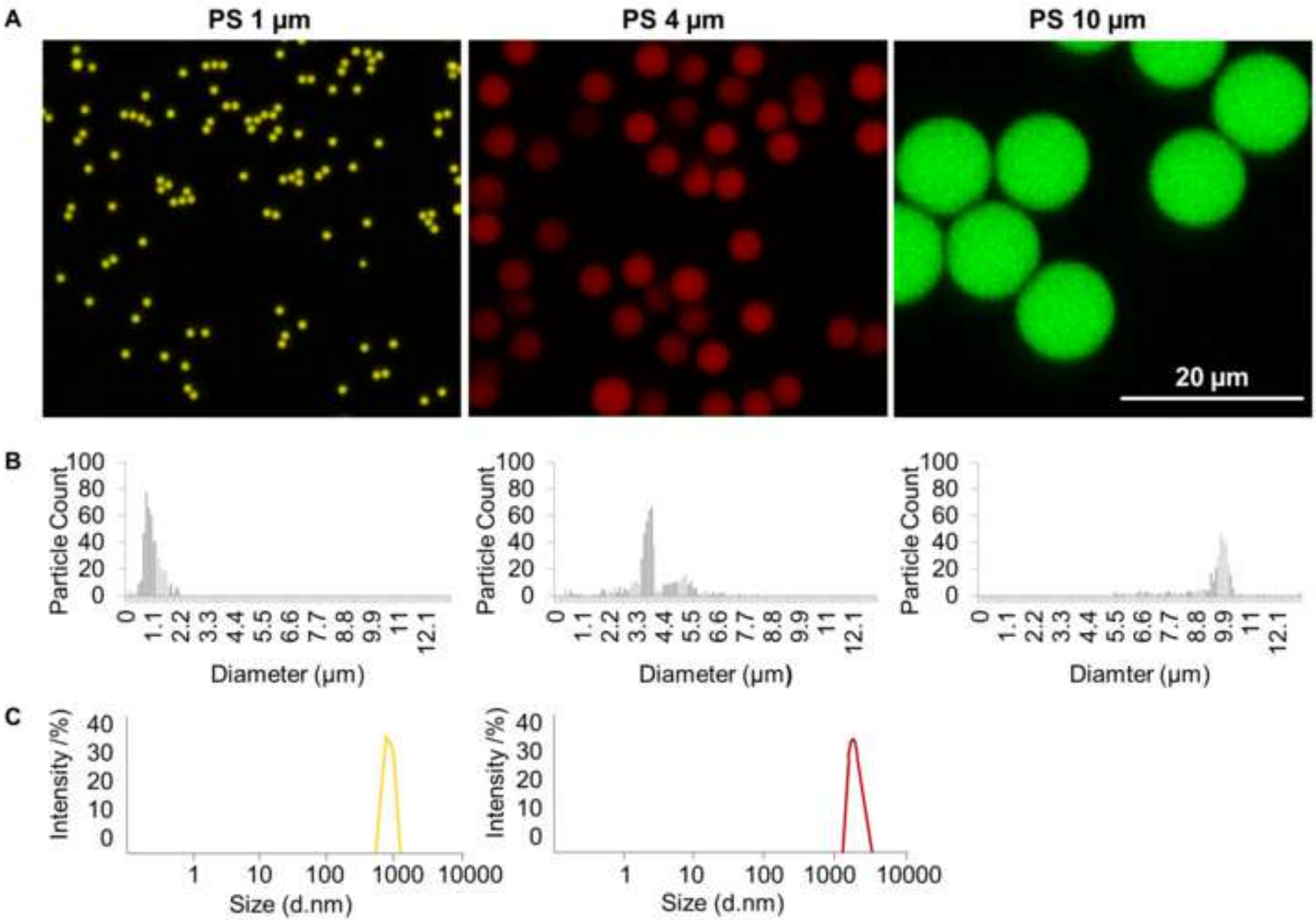

Figure 3

Click here to access/download;Figure;Figure 3_ANOVA.tif

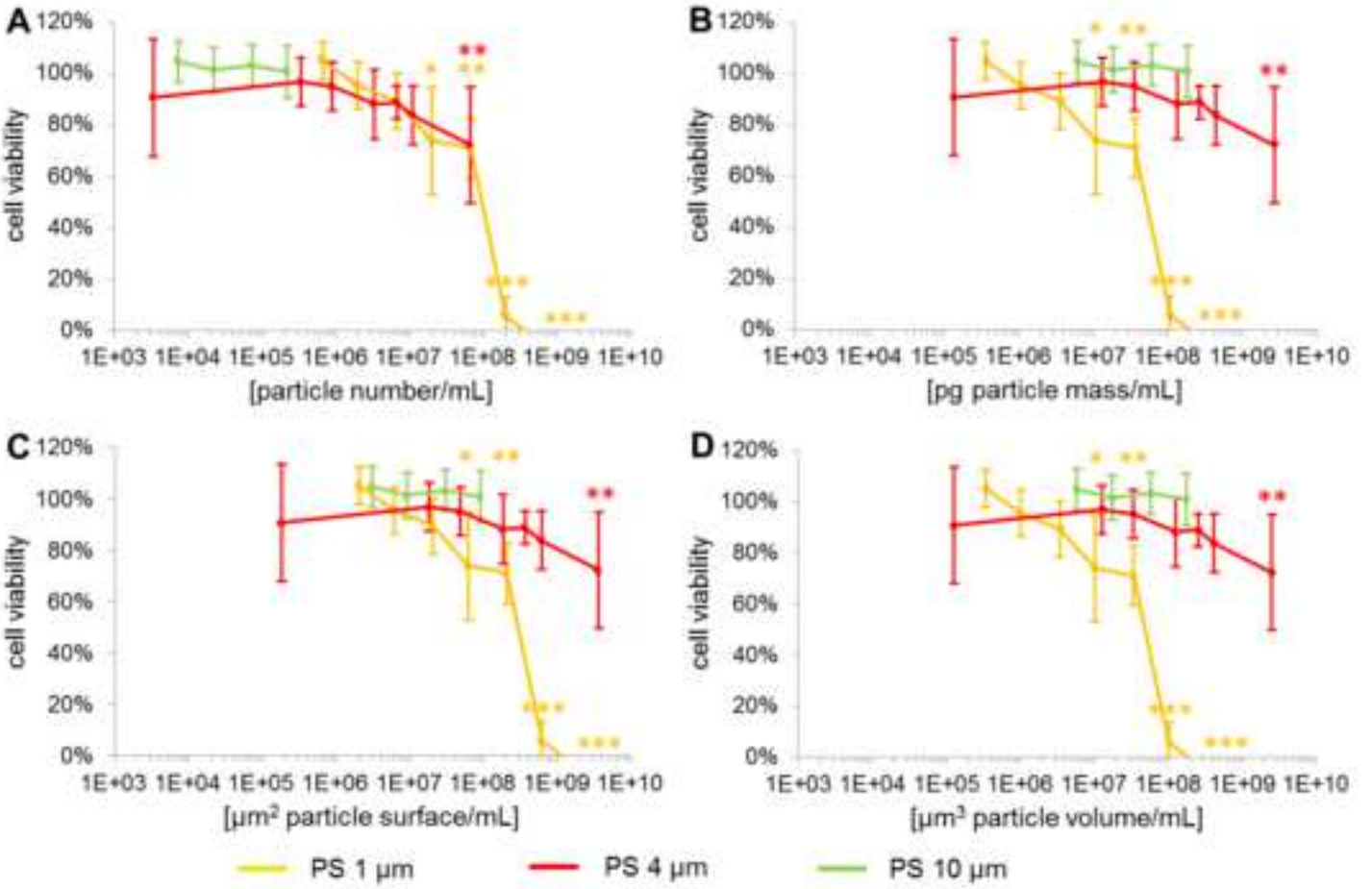

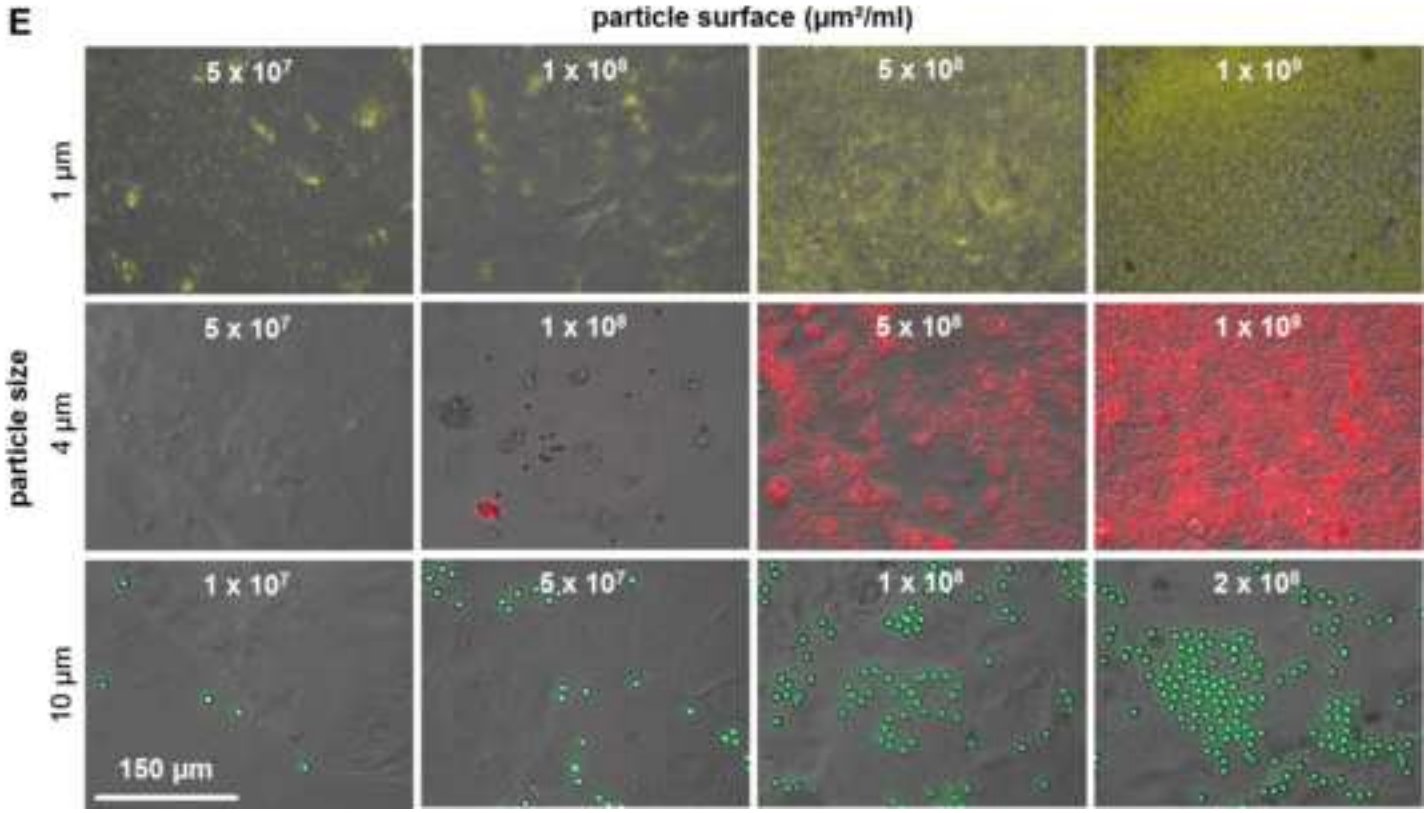

Figure 4

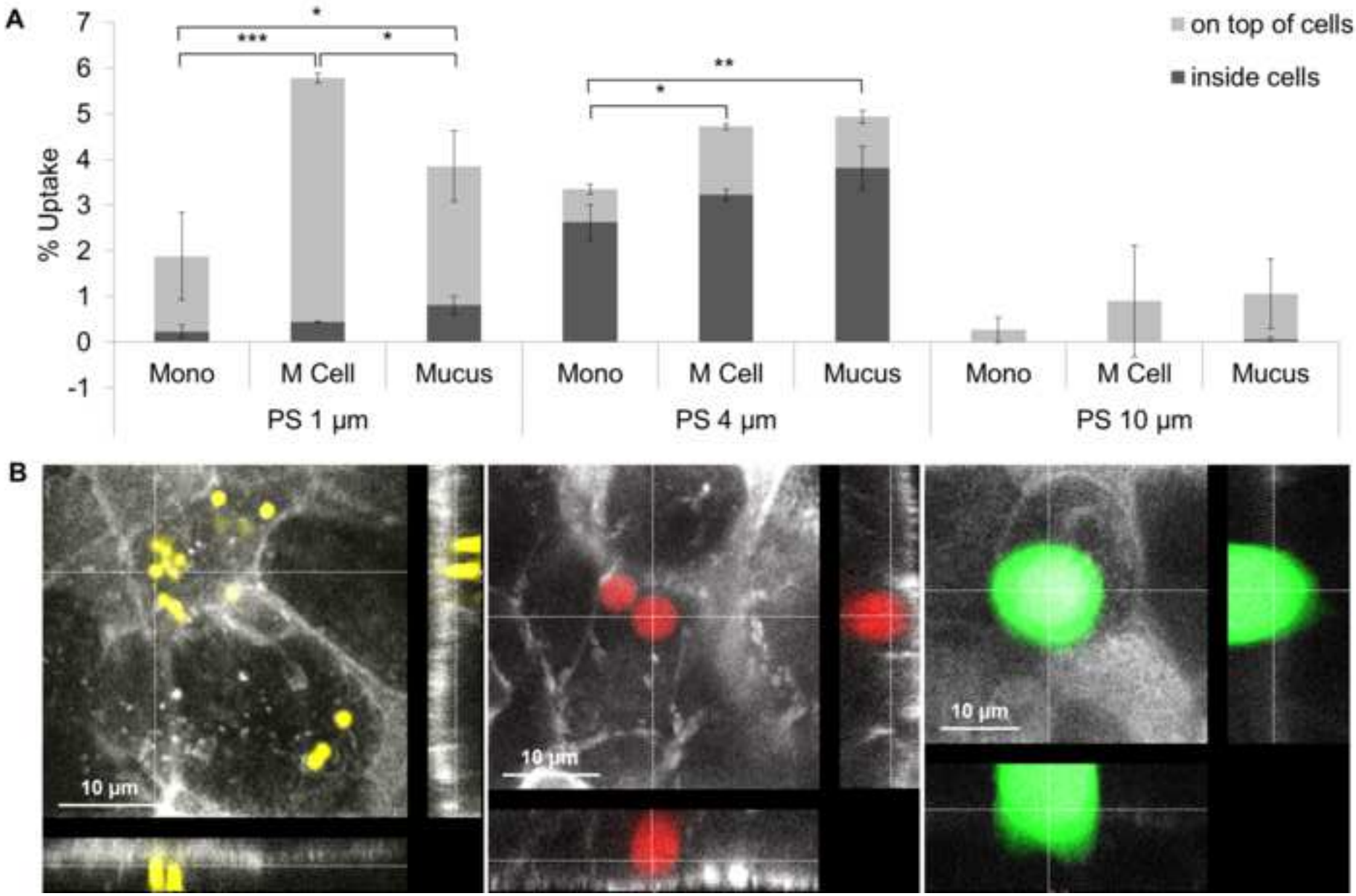

Figure 5

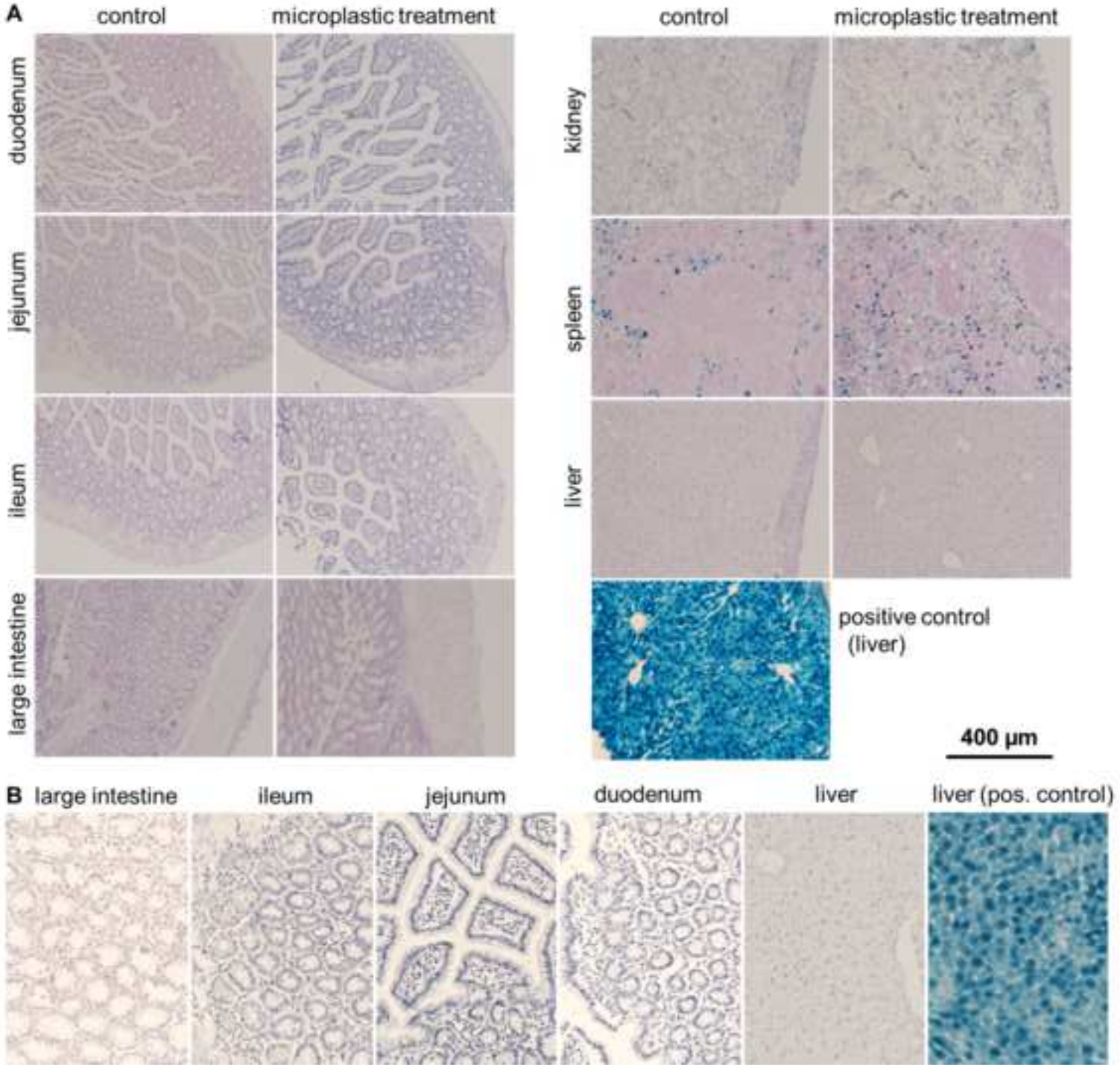

Figure 6

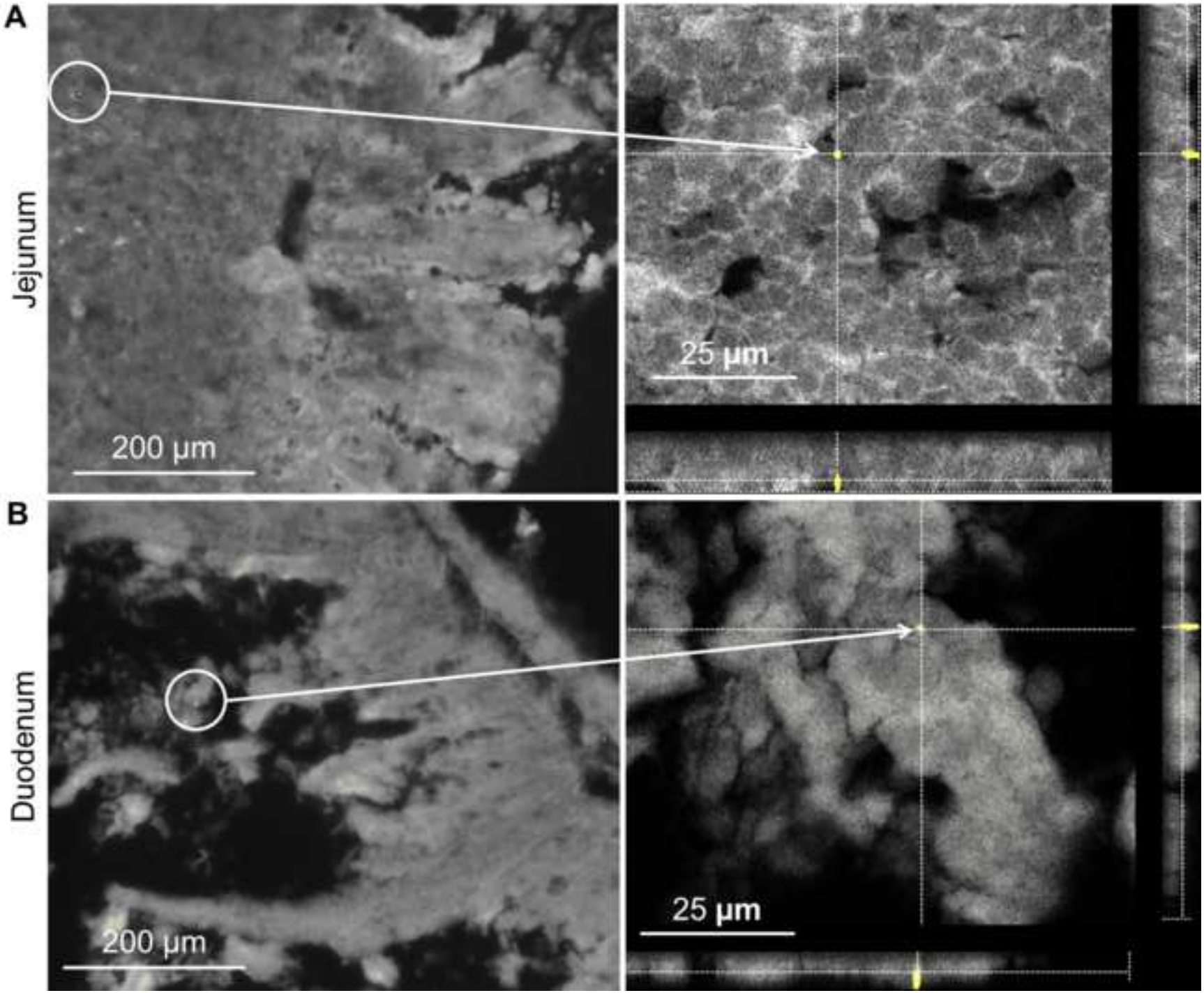

Figure 7

Click here to access/download;Figure;Figure 7_ANOVA.tif